Clays and Clay Minerals, Vol. 51, No. 2, 197–204, 2003.

ARSENIC SORPTION ONTO SOILS ENRICHED IN Mn AND Fe MINERALS

ELEONORA DESCHAMPS[1], VIRGINIA S. T. CIMINELLI[2,*], PETER G. WEIDLER[3] AND ALINE Y. RAMOS[4,†]

[1] State Environmental Agency-FEAM, Brazil
[2] Department of Metallurgical and Materials Engineering, Universidade Federal de Minas Gerais, UFMG, Brazil
[3] Institute for Technical Chemistry, Water- and Geotechnology (ITC-WGT), Forschungszentrum Karlsruhe-FZK, Germany
[4] Laboratório Nacional de Luz Síncrotron-LNLS/Campinas SP, Brazil

Abstract—The As sorption capacity of a natural Mn and Fe mineral-containing sample from the Iron Quadrangle province, Brazil, was investigated. A detailed mineralogical identification was obtained by combining X-ray diffraction analyses (with Rietveld refinement), X-ray fluorescence spectroscopy, optical microscopy, and scanning electron microscopy coupled with X-ray energy dispersive spectrometry-EDS. The oxidation state of the adsorbed As species was determined by X-ray absorption near edge structure spectroscopy. The results demonstrate that the presence of naturally occurring Mn oxides promotes the effective oxidation of As (III) to As(V). Also, the Mn minerals show a significant uptake of both the trivalent and pentavalent As species. This study demonstrates that the combined influences of As(III) depletion by oxidation and adsorption on a natural oxide sample consisting of Mn minerals and Fe oxides may effectively contribute to the reduction the As concentration in waters.

Key Words—Adsorption, Arsenate, Arsenic, Arsenite, Fe Oxides, Mn Oxides, XANES.

INTRODUCTION

Arsenic has been prominent in discussions about drinking water quality over the last decade. The drinking water limits for As decreased worldwide, following World Health Organisation (WHO) recommendations. One of the main factors controlling As concentration in natural aquatic systems is its adsorption onto the sediments, which promotes the immobilization of this metalloid. The processes that influence As adsorption at the water/mineral interfaces play an important role in the environmental biogeochemistry of As.

Recently, the potential health risk to local populations from As exposure has been established in gold-mining areas in the Iron Quadrangle mineral province, MG, Brazil (Matschullat *et al.*, 2000). In 1998, 126 schoolchildren aged 10 had their urine sampled. Twenty per cent of the total sample population showed As concentrations at a level (>40 μg^{-1}) for which adverse health effects cannot be excluded on a long-term basis. The hydrothermal gold deposits occurring in these areas contain varying proportions of Au-bearing sulfides, such as pyrite (FeS_2), pyrrhotite ($Fe_{1-x}S$) and arsenopyrite (FeAsS). Particularly high As concentrations in water (0.4–350 $\mu g\ L^{-1}$, median 55 $\mu g\ L^{-1}$), in soil (200–860 mg kg^{-1}, median 113 mg kg^{-1}), sediments (22–3200 mg kg^{-1}, median 350 mg kg^{-1}) and tailings (300–21000 mg kg^{-1}, median 10500 mg kg^{-1}) indicated possible pathways for As dispersion in the investigated area. As suggested by Matschullat *et al.* (2000), these concentrations are, in principle, explainable via weathering of mine waste and tailings and via smelting activities.

Arsenic toxicity, mobility and bioavailability in soil-water systems are highly dependent on its oxidation state and chemical speciation. Two inorganic forms of As, arsenite As(III) and arsenate As(V), are the main species in soils and sediments. The reduced state, As(III), is much more toxic (Ferguson and Davis, 1972), soluble and mobile than the oxidized form, As(V). This fact is related to the different adsorption behavior of these two species on soils. It is known that the mineral surface may either catalyze the redox reaction or act as a direct oxidant for As. The surface of Fe and Mn oxihydroxides are the major sources and sinks of As and other trace elements (Sung and Morgan, 1981).

A number of investigations have focused on As immobilization by natural and synthetic Fe oxides and Fe hydroxides (Isaacson *et al.*, 1994; Pierce and Moore, 1982; Davis and Leckie, 1980; Fuller *et al.*, 1993; Fendorf *et al.*, 1997; Ladeira and Ciminelli, 1998, 2000; Ladeira *et al.*, 2001). Fewer investigations have focused on As immobilization by Mn oxides (Nishimura and Umetsu, 1994; Driehaus *et al.*, 1995; Scott and Morgan, 1995). Investigations on samples containing both Mn and Fe minerals are reported even less frequently (Sun and Doner, 1998; Sun *et al.*, 1999) and in both cases have been carried out with synthetic materials. Recent studies (Waychunas *et al.*, 1993, 1995; Manceau, 1995; Sun and Doner, 1996; Fendorf *et al.*, 1997) indicate that Fe oxides may strongly adsorb As(V) by forming binuclear complexes. On the other hand, Mn oxides are effective oxidants for the transformation of As(III) into As(V) (Oscarson *et al.*, 1981; Moore, 1990; Scott and Morgan, 1995).

* E-mail address of corresponding author:
ciminelli@demet.ufmg.br
† Present address: LMCP, UMR7590 CNRS, France
DOI: 10.1346/CCMN.2003.0510210

X-ray adsorption near edge structure spectroscopy (XANES) is a direct method of determining the oxidation states of elements such as As and Mn. Different oxidation states of an element present different electron bonding energies. The energies of the edge peak increase with increasing oxidation state (Sun *et al.*, 1999). The edge shift between As(III) and As(V) in XANES spectra is large enough to determine As(III) and As(V) in a soil sample with unknown As oxidation states (Foster *et al.*, 1998).

This study investigates the As immobilization capacity of natural Mn and Fe minerals from the Iron Quadrangle, historically the most important Au- and Fe-producing province in Brazil. The results obtained through physicochemical and mineralogical characterization of a naturally occurring Fe and Mn oxide sample were supported by the results obtained with relatively pure natural samples consisting of Fe and Mn oxide phases. The XANES spectroscopy was applied to determine the oxidation state of As on these mineral soil samples and to investigate the ability of Mn minerals to promote the oxidation of As(III) to As(V). In a world of diminishing soil and water resources, the identification of sorbents that can be used in the remediation of contaminated sites assumes a greater importance than ever before.

MATERIALS AND METHODS

Investigations were performed on a complex sample consisting of Fe/Mn oxides (cFeMn) collected at the Iron Quadrangle. Additionally, relatively 'pure' samples of Fe and Mn minerals were selected in the same region and studied in order to establish a correlation between the behavior of the complex Fe/Mn oxide sample and that of its more abundant constituents. The cFeMn sample was supplied by Extramil S/A (Santa Barbara, Brazil) and was used in this study without pretreatment (100% <45 μm). Fine-grained samples of goethite (Gt) and hematite (Hm) were supplied by Minerações Brasileiras Reunidas (Nova Lima, Brazil). After dry sieving (nylon mesh 45 μm), the fine fraction was used for subsequent analyses. Coarser material, if present, was discarded. The enriched Mn oxide samples, todorokite/pyrolusite (Td/Py) and todorokite/birnessite (Td/Bn) were supplied by Mineração Conselheiro da Mata Ltda (Conselheiro da Mata, Brazil). The samples were ground and sieved at 45 μm, the coarse fraction being discarded.

The chemical composition of the samples was determined by wet chemistry methods. Silica was determined via weight loss after treatment with hydrofluoric acid. Manganese was determined by means of potentiometry using K permanganate and Na pyrophosphate. Iron was determined by titration with K permanganate. Sodium, Al, Ti and Mg were determined by atomic absorption spectometry (AAS) (Perkin Elmer model Analyst 300) after digestion in HNO_3/HCL solution (Young, 1971). The mineralogical composition of the samples was identified by combining optical microscopy (Leitz model Labor Lux 12 Pols) with X-ray fluorescence analysis (XRF) (Philips model PW2510), scanning electron microscopy (SEM) (Jeol model JSM35C) coupled with X-ray energy dispersive spectrometer-EDS (Voyager model 1050), and X-ray powder diffraction (XRD, Siemens model D5000).

The XRD measurements were performed on a Siemens diffractometer equipped with a rotating anode (MoK_1, λ = 0.70926 nm) in Bragg-Brentano geometry. The powder sample was pressed gently into the indentation of a holder to prevent orientation of the particles. Five per cent by weight of LaB_6 was added as an internal standard. The diffraction patterns were recorded over an angular range of 2–35°2θ and counting time varied for the different samples from 5–20 s per 0.01°2θ step. To determine the mineral composition of the multimineral cFeMn-sample, a sequential dissolution procedure with boiling HCl and HCl at room temperature was applied. After each dissolution step the sample was X-rayed. The Rietveld method was applied to estimate the mineral content (Young, 1993; Weidler *et al.*, 1998). Full refinement could not be successfully applied to the untreated sample due to the massive peak overlap and thus difficulties in applying the correct profile function. In addition, an elemental composition of the Mn-bearing phases was assumed as found in Burns (1979). The mineral content determined by XRD was compared to that indicated by chemical analysis, thus yielding the most probable mineral composition for the Mn oxides and of the entire sample. The XRD data of the partially dissolved cFeMn sample was considered for the determination of Al substitution of the Fe phases following the approach of Schwertmann and Carlson (1994) for goethite and of Stanjek and Schwertmann (1992) for hematite.

Physical properties like particle-size distribution were measured by wet sieving combined with a sedimentation technique (Micromeritics, model Sedigraf 5000ET); the specific surface areas were calculated by the BET equation using a multiple point technique (Quantachrome model NOVA1000). The sample was degassed at 70°C for 2 h with a continual stream of N_2 prior to the surface area determination.

Total As in solution and soil samples was determined after digestion by ICP-AES (Spectro, model Modula). Prior to digestion 500 mg of dry material was mixed with 15 mL of deionized water, 3 mL of HCl and 1 mL of HNO_3. The samples were digested in a microwave oven (Maasen, model MWS) in 80 mL PTFE vessels. The temperature was maintained for 20 min at 175°C. The resulting pressure was ~2.5×10^6 Pa. After cooling, the digested samples were transferred to 25 or 50 mL flasks, and these were filled with deionized water. The samples were stored in 50 mL polypropylene (PP) bottles the until ICP measurements.

https://doi.org/10.1346/CCMN.2003.0510210 Published online by Cambridge University Press

Table 1. Chemical composition of the cFeMn sample.

Oxides	Fe_2O_3	MnO_2	SiO_2	Al_2O_3	K_2O	CaO	MgO	Ti	LOI
Wt.%	36.2	32.6	8.7	6.8	0.7	0.2	0.7	0.3	13.4

LOI = loss on ignition at 900ºC

Sorption isotherms

The trivalent and pentavalent As solutions were prepared by dissolving reagent-grade sodium (meta) arsenite ($AsNaO_2$ PA; >99.0%; Fluka) and di-sodium hydrogen arsenate heptahydrate ($Na_2HAsO_4.7H_2O$ PA; >98.5%, Fluka), respectively, in deionized Milli-Q water. To obtain the sorption isotherms, experiments were performed with the cFeMn sample and with the Gt, Hm, Td/Py and Td/Bn samples at selected pH values adjusted with NaOH or HCl. The solid sample (10 g) and 100 mL of As solution (concentrations of 100 to 2000 mg/L) were shaken for 24 h, at a constant temperature (25±0.5ºC) and pH. The pH was checked each hour and corrected whenever necessary. After 24 h the pH was measured and samples were filtered for the determination of As. Replicates were prepared for randomly chosen tests.

XANES measurements

The As(III)- and As(V)-treated samples were mounted in Teflon cells and sealed with thin Kapton polyamide film to minimize X-ray absorption. The X-ray absorption measurements were performed at the XAS beam line of the Laboratório Nacional de Luz Síncrotron (LNLS, Campinas, Brazil) (Tolentino *et al.*, 2001). The LNLS storage ring is a third-generation machine operating at 1.37 GeV with nominal ring current of 130 mA. X-absorption data were collected at the As K-edge (11870 eV) in the fluorescence mode. The incident beam was monitored by an air-filled ion chamber. The fluorescence beam was detected using a NaI scintillator with Ge filter to limit the contribution of the scattering beam. An air-filled ion chamber monitored the incident beam monochromatized with a 'channel-cut' Si (111) monochromator. The overall resolution was 3.4 eV, including core hole level (2.1 eV) and instrumental resolution (2.7 eV). The energy was calibrated at the inflection point of edge jump in the XANES spectrum of As(0) (11867 eV). All XANES spectra were collected in the range 11820 to 12020 eV with an energy step of 0.8 eV from 11850 to 11929 eV and 2 eV beyond this interval. The collecting time was from 6 to 12 s per point, depending on the As ratio in the sample. The energy stability was checked to be better than 0.1 eV during all measurements. The experimental XANES spectra were background-corrected using a polynomial fit in the region before the pre-edge and normalized in the range 11950–12030 eV. After these operations the edge features are directly comparable in position and intensity.

RESULTS AND DISCUSSION

Characterization of the FeMn sample

The chemical composition of the cFeMn sample is shown in Table 1. The Fe and Mn appear as the main constituents followed by silica and aluminum. Traces of K, Ca, Mg, Na and Ba have also been identified by XRF analyses. The particle-size analyses indicated a very fine sample, with 95% of the particle sizes <15 μm and 50% <2 μm.

Observation of the sample under an optical microscope indicated the presence of goethite, hematite, magnetite (as Fe sources) and quartz. The most abundant constituents of the sample (Figure 1) were round aggregates probably originating from the alteration of FeMg silicates. The characteristic variety of Mn oxyhydroxides, textural peculiarities of the sample, such as intergrowth structures and fine grain size made particularly difficult the complete identification of the sample constituents under the microscope. The diagnosis was completed by XRD analysis. The elemental composition of a typical aggregate, presented in Figure 1, indicates the predominance of Fe and Mn, with traces of Al, Si, K, Ba and Ca.

Figure 2 shows the XRD patterns of the untreated and the acid-treated cFeMn sample. The vertical bars represent the peak positions of the noted minerals. Figure 2 indicates the presence of nine different minerals (LaB6 was used as internal standard): hematite (ICCD 33-0664), goethite (ICCD 29-0713), todorokite (ICDD 21-0553), birnessite (ICDD 890-1098), cryptomelane (ICCD 44-1386), lithiophorite (ICCD 41-1378), quartz (ICCD 46-1045), kaolinite (ICCD 80-0886), and muscovite (ICCD 76-0929).

Other mineral phases were detected after a magnetic separation. The XRD pattern of the concentrate revealed the presence of magnetite and maghemite in close relation to hematite. The magnetite and maghemite

Table 2. Mineralogical composition of the cFeMn sample by Rietveld refinement and chemical analysis.

Mineral	Wt.%
Goethite ((FeO(OH))	30
Hematite (αFe_2O_3)	19
Todorokite ($(Ca,Na,K)(Mg,Mn^{2+})Mn_5O_{12}.xH_2O$)	6
Cryptomelane ($K_{2-x}Mn_8O_{16}$)	15
Birnessite ($(Na,Ca,K)(Mg,Mn)Mn_6O_{14}.5H_2O$	13
Lithiophorite ($AlLiMnO_2(OH)_2$)	2
Quartz (SiO_2)	7
Muscovite ($(K,Na)(Al,Mg,Fe)_2(Si_{3.1}Al_{0.9})O_{10}(OH)_2$)	8

https://doi.org/10.1346/CCMN.2003.0510210 Published online by Cambridge University Press

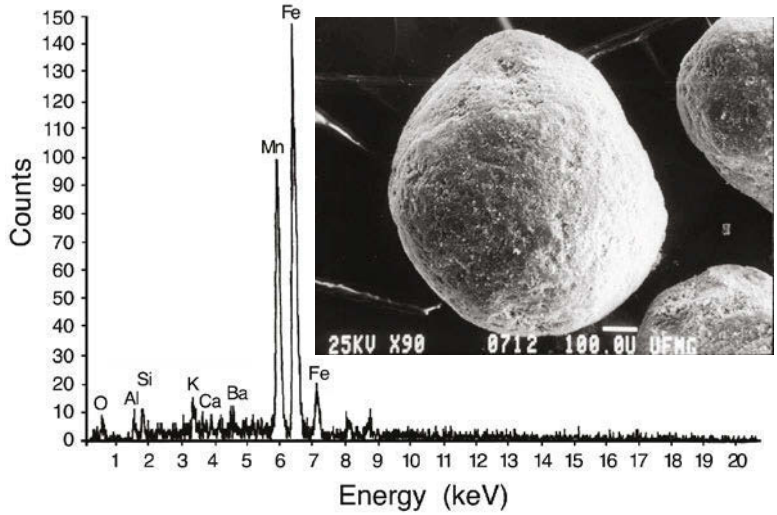

Figure 1. SEM micrographs and elemental composition (EDS) of typical rounded aggregates in the cFeMn sample.

amounted to only traces as estimated by comparison with the results of the untreated cFeMn sample.

The relative proportions of the crystalline phases, which constitute the cFeMn sample, were determined by Rietveld refinement of the powder XRD patterns. In fact, variations in the chemical composition are the norm with complex Mn oxides and can be explained easily by the manifold substitution of the cations. The deviations from stoichiometry are based on the easy substitutability of the cations and the water in the interlayers (Varentsov, 1964). Table 2 shows the mineralogical composition of the sample. Cryptomelane is the most common Mn oxide and accommodates K in the tunnels which are formed by corner-sharing double chains of octahedra. The composition is not constant and for the present sample corresponds to the formula $K_{2-x}Mn_8O_{16}$. For todorokite, the suggested formula based on the chemical composition and on the XRD patterns, shown in Figure 2, is $(Ca,Na,K)(Mg,Mn^{2+})Mn_5O_{12}.xH_2O$, for lithiophorite is $AlLiMnO_2(OH)_2$ and for birnessite is

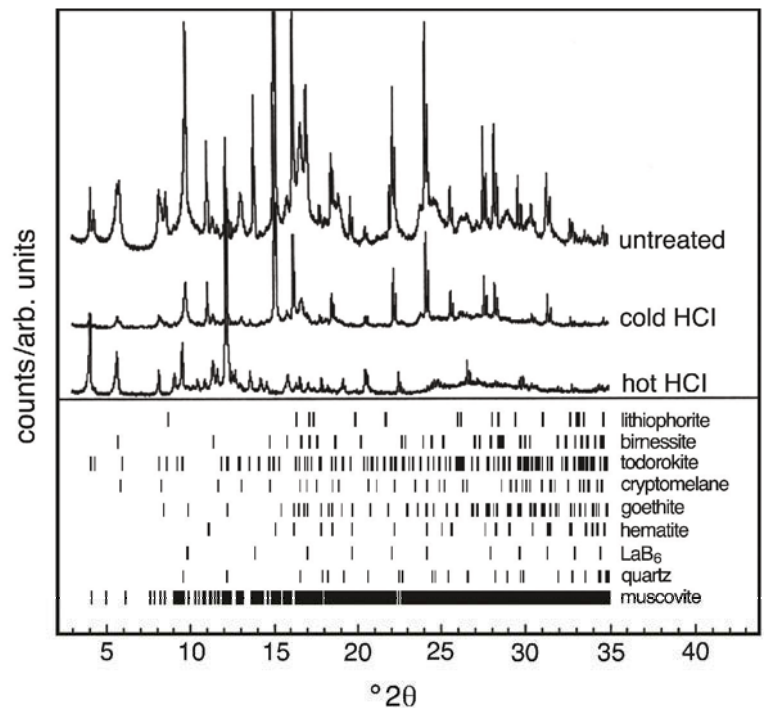

Figure 2. XRD pattern of the untreated and acid-treated cFeMn sample. The vertical bars indicate the peak positions of the minerals denoted on the right.

https://doi.org/10.1346/CCMN.2003.0510210 Published online by Cambridge University Press

$(Na,Ca,K)(Mg,Mn)Mn_6O_{14}.5H_2O$. The dissolution in boiling HCl dissolved the Fe- and Mn-bearing mineral phases, leaving quartz (~45 wt.%), kaolinite (~40 wt.%) and muscovite (~15 wt.%) in the sample. Treatment with HCl at room temperature dissolved all Mn-bearing mineral phases. The quartz content was ~3 wt.%, kaolinite 13 wt.%, muscovite 6 wt.%, hematite 35 wt.% and goethite 43 wt.%. The Rietveld refinement yielded precise unit-cell parameters for goethite and hematite which allowed the determination of Al substitution. The difference between these refined unit-cell parameters and those of unsubstituted hematite yields an Al substitution of ~0.5 mol.%, *i.e.* an almost Al-free hematite in the sample. For goethite the substitution was ~15 mol.%, thus indicating that goethite was formed in an Al-rich environment as found in weathering zones. That is in agreement with the study by Schulze (1984) of the influence of Al on Fe oxides. The author determined the Al substitution on goethite, with a maximum observed in synthetic and natural samples as high as 33%.

Based on the mineralogical composition of the cFeMn sample, relatively 'pure' minerals were selected from the same mineral province and investigated using XRF followed by XRD. In the case of Mn minerals, the results (XRD patterns not shown here) indicated that the samples contained two main Mn phases, todorokite with minor birnessite (Td/Bn) in one and todorokite and minor pyrolusite (Td/Py) in the other. Goethite (Gt) and hematite (Hm) represented the Fe oxide phases. Considering all selected samples, the relatively 'pure' mineral samples investigated in the present study were identified (on a weight basis) as: Gt (Fe_2O_3 69.1%, SiO_2 14.4%, Al_2O_3 3.3%), Hm (Fe_2O_3 97.3%), Td/Bn (MnO_2 71.0%, Al_2O_3 3.4%, Fe_2O_3 7.6%, SiO_2 2.6%), Td/Py (MnO_2 59.5%, Fe_2O_3 7.0%, SiO_2 7.7%, Al_2O_3 13.3%).

Loading

To determine the maximum As uptake (Q_{max}), sorption isotherms were constructed for the pentavalent and the trivalent As species. The experimental data from the sorption isotherms, well adjusted by the Langmuir equation (correlation coefficients of 0.98 for As(III) and 0.99 for As(V)) were used to calculate the Q_{max} values using the following equation:

$$Q = Q_{max} \cdot K \cdot C/(1+K \cdot C) \quad (1)$$

where Q is the uptake of As adsorbed by the sorbent (mg/g); Q_{max}, the maximum As uptake (mg/g); C, the equilibrium concentration of the As ion in the aqueous phase (mg/L) and K a constant.

Figure 3 shows the maximum As uptake by the cFeMn sample treated with As(V) or As(III), at selected pH values. The dependence of As removal on the solution pH was studied extensively and reported in the literature (Gupta and Chen, 1978; Pierce and Moore, 1982; Gosh and Yan, 1987; Zouboulis and Kydros, 1993; Mortazavi *et al.*, 1993). Changes in the solution pH greatly affect the sorption process. For As(V) the maximum uptake of 7.7 mg/g and 6.8 mg/g, as indicated by Figure 3, occurred in acid conditions (pH 3.0–5.5), and decreased to 4.0 mg/g with increasing pH values (pH 8.0). According to thermodynamics, the anionic monovalent species ($H_2AsO_4^-$) predominates at pH 2.3 to 7.0 ($pKa_1 = 2.3$) and the anionic divalent species, ($HAsO_4^{2-}$), at pH >7 ($pKa_2 = 7.0$).

The same trend was observed with the trivalent species. As indicated by Figure 3, an increasing pH decreases As uptake, which reached 9.2 mg/g, at pH 3.0, 9.1 mg/g at pH 5.5 and 6.3 mg/g at pH 8.5. Under mildly reducing conditions, the predominant As(III) species for pH 3.0 to 5.5 are the neutral (H_3AsO_3) molecule and at pH 8.0 the anionic monovalent species, ($H_2AsO_3^-$). Summarizing, Figure 3 shows a similar trend for both the trivalent and pentavalent species, which means that the sorption process is favored by the decrease in pH.

The adsorption of As(III) and As(V) on goethite as a function of pH has been studied by many authors (Sun and Doner, 1998; Pierce and Moore, 1980, 1982; Ferguson and Anderson, 1974). In all these studies, maximum As(V) uptake occurred under acid conditions and decreased with increasing pH. In agreement with these findings, the results shown in Figure 3 indicated the greatest uptake at pH 3.

The adsorption of As(III), on the other hand, is not consistent with previous findings which indicated an increase in As uptake with pH. The results depicted in Figure 3, showing the same trend for both the pentavalent and trivalent species, suggested that the presence of Mn minerals in the sample promoted the oxidation of As(III) to As(V). As a result, the adsorption envelopes of As(III) and As(V) became quite similar. This is in agreement with the work by Sun and Doner (1998), showing that the addition of 0.5% of birnessite (w/w of goethite) to the As(III)-goethite system completely depleted As(III) in solution within 50 min at both pH 5.0 and pH 8.0. The addition of birnessite perturbs the equilibrium ratio of As(III) to As(V) in solution.

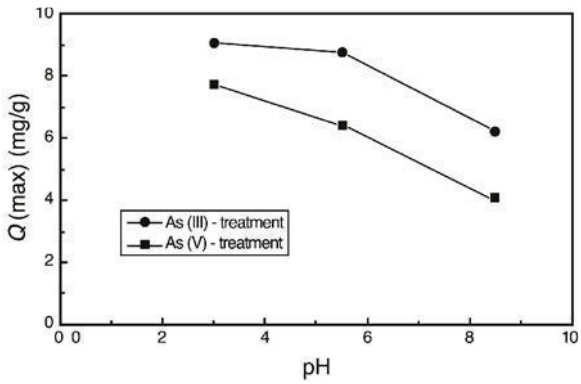

Figure 3. Maximum As uptake for the cFeMn sample treated with As(III) or As(V) at selected pH values.

https://doi.org/10.1346/CCMN.2003.0510210 Published online by Cambridge University Press

Consequently, more As(III) will be desorbed from the goethite surface, oxidized by birnessite in the solution and then readsorbed as As(V). The greater uptake shown by the As(III)-treated samples in Figure 3 is not fully understood at this point. Current investigations using extended X-ray absorption fine structure (EXAFS) suggest that different sites may be involved in the uptake of As(III) and As(V).

Table 3 lists the As uptake by the cFeMn sample and by the relatively 'pure' sample treated with As(III) and As(V), respectively, and their specific surface areas. The smallest surface areas are shown by hematite and goethite followed by todorokite/pyrolusite, whereas the cFe/Mn sample presented the largest surface area (40.8 m^2/g) of all the studied samples. Conversely, the greatest loading is shown by goethite and by hematite, whereas the cFeMn sample displayed the lowest (As(V)) or the second lowest (As(III)) loading. These results suggest a relatively larger affinity for As(III) by the Fe oxides.

XANES analyses

The energy at which an absorption edge occurs is characteristic of the absorbing element, but the exact position of the edge varies as a function of the oxidation state of the element. The loss of an electron by oxidation causes the remaining electrons to be bound more tightly by the nucleus. Thus, greater X-ray energy is required to remove the remaining electrons and the X-ray absorption edges shift to higher energies by ~2 or 3 eV for each electron lost. In principle, the oxidation state of an element can be deduced from the energies of the XANES spectral features (Waychunas *et al.*, 1993).

Table 3. As uptake by natural Fe and Mn mineral samples treated with As(III) and As(V) and their specific surface areas.

Mineral sample	Specific surface area (m^2/g)	As(III) (μmol/m^2)	As(V) (μmol/m^2)
Hematite	2.2	4.9	5.3
Goethite	7.9	5.1	4.5
Todorokite/birnessite	13.8	3.3	5.0
Todorokite/pyrolusite	8.6	2.4	4.3
cFeMn sample	40.8	2.9	2.1

Loading conditions: pH = 5.5, Ionic strength = 0.15, initial concentration = 1000 mg/L

The spectroscopic technique XANES was applied to investigate the oxidation of As(III) to As(V) by goethite, todorokite/birnessite, todorokite/pyrolusite and by the cFeMn sample. Arsenic K XANES spectra of the samples treated with As(III) and As(V) are shown in Figure 4. As(III) has an edge peak at ~11,872 eV, whereas As(V) has an edge peak at ~11876 eV, with a shift of ~4 eV. Figure 4 shows that the As(III)-treated goethite displays an edge-peak at 11873 eV. This position corresponds to a three-fold formal valency for the As (Foster *et al.*, 1998), thus indicating that no oxidation occurs with As(III) in contact with goethite sample. Conversely, the positions of the absorption edge are the same in the As(III)- and As(V)-treated todorokite/birnessite as well as todorokite/pyrolusite samples. This finding indicates that the Mn minerals are strong oxidants for As(III). These results are in agreement with the investigations of Sun *et al.* (1999), and also with Manning *et al.* (1998). Using XANES and solution chemical methods, Sun *et al.* (1999) studied the

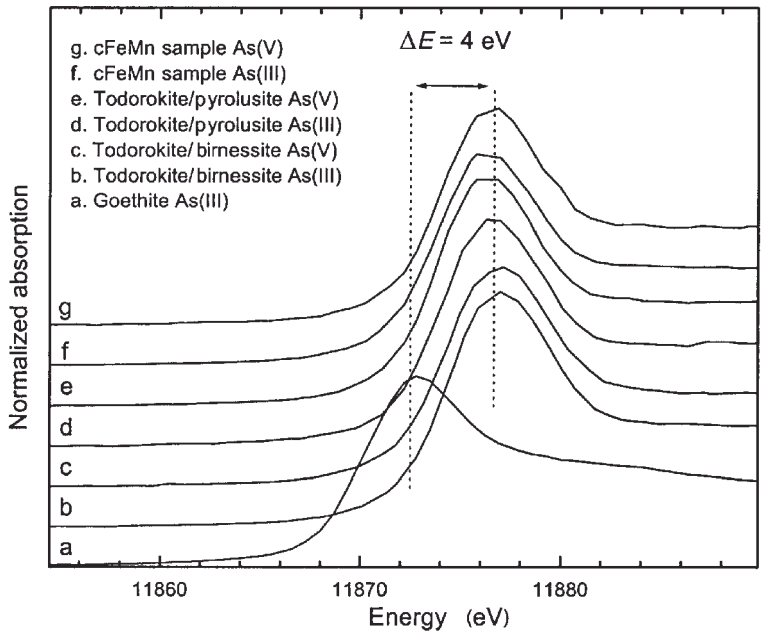

Figure 4. Normalized As K XANES spectra of As(III) and As(V) adsorbed on the cFeMn sample, and on goethite, todorokite/pyrolusite and todorokite/birnessite samples.

https://doi.org/10.1346/CCMN.2003.0510210 Published online by Cambridge University Press

interaction between As(III) and Mn-substituted goethite. They found that the oxidation of As(III) increased with increased Mn substitution in goethite. Manning *et al.* (1998) studied the adsorption and stability of As(III) on goethite using combinations of standard batch techniques and X-ray absorption spectroscopy (XAS). They found that all As(III)-treated α-FeOOH samples investigated showed energy positions indicative of As(III), thus suggesting that oxidation to As(V) on the α-FeOOH surface had not occurred.

In the present investigation, evidence from XANES analyses indicated that all the naturally occurring Mn minerals have a profound influence on the oxidation of As(III) to As(V). These results suggest the important role of the combined effect of Fe and Mn oxyhydroxides on the availability and toxicity of As in the environment.

CONCLUSIONS

The mineralogical composition of the soil enriched with Mn and Fe minerals indicated the presence of nine different minerals: hematite, goethite, todorokite, birnessite, cryptomelane, lithiophorite, quartz, kaolinite and muscovite.

Sorption experiments showed maximum uptake at pH 5.5 of 6.8 and 9.1 mg As g^{-1} of the cFeMn sample for As(V) and As(III), respectively, estimated by fitting Langmuir equations. The sorption process was favored by the decrease in pH for both the trivalent and the pentavalent species. These results suggested that the presence of Mn minerals in the sample promoted the oxidation of As(III) to As(V).

XANES spectroscopy was used to investigate the oxidation of As(III) to As(V) on the cFeMn sample surface. The results indicated, for the first time, the effective oxidation of As(III) to As(V), in contact with naturally occurring todorokite, birnessite, cryptomelane and pyrolusite minerals. Equally important is the fact that, though not as high as those depicted by the Fe minerals, significant adsorption of both the trivalent and pentavalent As species is shown by the Mn minerals. Finally, this study demonstrates that the oxidation-adsorption system composed of Mn minerals (todorokite, birnessite, cryptomelane and lithiophorite) and Fe oxides (goethite, hematite and magnetite) may be an important means of altering the As toxicity in terrestrial environments.

ACKNOWLEDGMENTS

The authors are grateful to Wolfgang Höll, for the use of the ITC-WGT facilities at Forschungszentrum Karlsruhe, Germany and to Dr Hannelore Bernotat for recording the XRD patterns. We also thank Humberto Terrazas Salas (Centro de Desenvolvimento da Tecnologia Nuclear-CDTN/CNEN, Belo Horizonte, Brazil) for his help in the mineralogical characterizatio n, and Jörg Matschullat (Freiberg University of Mining and Technology, Germany) for his critical comments. Finally we acknowledge the contribution of the National Synchrotron Light Laboratory (LNLS), Campinas, Brazil in performing the XANES experiments and CNPq. The authors wish to acknowledge the substantive reviews by Harvey Doner, Helge Stanjek and an anonymous reviewer.

REFERENCES

Burns, R.G. (editor) (1979) *Marine Minerals.* Short Course Notes, **6**. Mineralogical Society of America, Washington, D.C., 380 pp.

Davis, J.A. and Leckie, J.O. (1980) Surface ionization and complexation at the oxide/water interface. 3 Adsorption of anions. *Journal of Colloid and Interface Science*, **74**, 32–43.

Driehaus, W., Seith, R. and Jekel, M. (1995) Oxidation of arsenate(III) with manganese oxides in water treatment. *Water Research*, **29**, 297–305.

Fendorf, S., Eick, M.J., Grossl, P. and Sparks, D.L. (1997) Arsenate and chromate retention mechanisms on goethite. 1. Surface structure. *Environmental Science & Technology*, **31**, 315–320.

Ferguson, J.G. and Anderson, M.A. (1974) Chemical form of arsenic in water supplies and their removal. *Proceedings of the Symposium of Chemical Water Supply, Treatment and Distribution*, pp. 137–158.

Ferguson, J.G. and Davis, J. (1972) A review of the arsenic cycle in natural waters. *Water Resources*, **6**, 1259–1274.

Foster, A.L., Braun, G.E., Jr., Tingle, T.N. and Parks, G.A. (1998) Quantitative arsenic speciation in mine tailings using X-ray absorption spectroscopy. *American Mineralogist*, **83**, 553–568.

Fuller, C.C., Davis, J.A. and Waychunas, G.A. (1993) Surface chemistry of ferrihydrite: Part 2. Kinetics of arsenate adsorption and coprecipitation. *Geochimica et Cosmochimica Acta*, **57**, 2271–2282.

Gosh, M.M. and Yuan, J.R. (1987) Adsorption of inorganic arsenic and organoarsenicals on hydrous oxides. *Environmental Progress*, **6**, 150–157.

Gupta, S.K. and Chen, Y.K. (1978) Arsenic removal by adsorption. *Journal of Water Pollution Control Federation*, **50**, 493–506.

Isaacson, A.E., Corwin, R.R. and Jeffers, T.H. (1994) Arsenic removal using immobilized ferric oxyhydroxides. Pp. 47–55 in: *Proceedings of the International Symposion on Impurity Control and Disposal in Hydrometallurgical Processes* (B. Harris and E. Krause, editors). CIM, Canada.

Ladeira, A.C. and Ciminelli, V.S.T. (1998) Arsenic immobilization by adsorption on clay minerals. Pp. 515–520 in: *Fundamentals of Adsorption,* Vol. **6** (F. Meunier, editor). Elsevier, France.

Ladeira, A.C. and Ciminelli V.S.T. (2000) Mobility of As(III) and As(V) in soils. Pp. 191–198 in: *Minor Elements 2000: processing and environmental aspects of As, Sb, Se, Te, and Bi* (C. Young, editor). SME-AIME, USA.

Ladeira, A.C.Q., Ciminelli, V.S.T., Alves, M.C.M., Duarte, H.A. and Ramos, A.Y. (2001) Mechanism of anion retention from EXAFS and density functional calculations: Arsenic (V) adsorbed on gibbsite. *Geochimica et Cosmochimica Acta*, **65**, 1211–1217.

Manceau, A. (1995) The mechanism of anion adsorption on iron oxides: Evidence for the bonding of arsenate tetrahedral on free $Fe(O,OH)_6$ edges. *Geochimica et Cosmochimica Acta*, **59**, 3647–3653.

Manning, B.A., Fendorf, S.E. and Goldberg, S. (1998) Surface structures and stability of arsenic(III) on goethite: spectroscopic evidence for inner-sphere complexes. *Environmental Science & Technology*, **32**, 2383–2388.

Matschullat, J., Borba, R.P., Deschamps, E., Figueiredo, B.F.,

Gabrio, T. and Schwenk, M. (2000) Human and environmental contamination in the Iron Quadrangle, Brazil. *Applied Geochemistry,* **15**, 181–190.

Moore, J.N., Walker, J.R. and Hayes, T.H. (1990) Reaction scheme for the oxidation of As(III) to As(V) by birnessite. *Clays and Clay Minerals*, **38**, 549–555.

Mortazavi, S., Volchek, K. and Whittaker, H. (1993) The removal of arsenic from water by adsorption and microfiltration. Pp. 9–29 in: *Proceedings of the 10th Technical Seminar on Chemical Spills*, St. John, New Brunswick, Canada.

Nishimura, T. and Umetsu, Y. (1994) Removal of arsenic(III), arsenic(V) with manganese from aqueous solution by ozonation. Pp. 91–100 in: *Proceedings of the International Symposium on Impurity Control and Disposal in Hydrometallurgical Processes* (B. Harris, and E. Krause, editors). CIM, Canada.

Oscarson, D.W., Huang, P.M., Defosse, C. and Herbillon, A. (1981) Oxidative power of Mn(IV) and Fe(III) oxides with respect to As(III) in terrestrial and aquatic environments. *Nature*, **291**, 50–51.

Pierce, M.L. and Moore, C.B. (1980) Adsorption of arsenite on amorphous iron hydroxide from dilute aqueous solution. *Environmental Science Technology*, **14**, 214–216.

Pierce, M.L. and Moore, C.B. (1982) Adsorption of arsenite and arsenate on amorphous iron hydroxide. *Water Research*, **16**, 1247–1253.

Schulze, D.G. (1984) The influence of aluminum on iron oxides. VIII. Unit cell dimensions of Al-substituted goethite and estimation of Al from them. *Clays and Clay Minerals*, **32**, 36–44.

Schwertmann, U. and Carlson, L. (1994) Aluminum influences on iron oxides: XVII. Unit cell parameters and aluminum substitution of natural goethites. *Soil Science Society of America Journal*, **58**, 256–261.

Scott, M.J. and Morgan, J.J. (1995) Reactions at oxide surfaces. Oxidation of As(III) by synthetic birnessite. *Environmental Science & Technology*, **29**, 1898–1905.

Stanjek, H. and Schwertmann, U. (1992) The influences of aluminum on iron oxides. XVI: Hydroxyl and aluminum substitution in synthetic hematites. *Clays and Clay Minerals*, **40**, 347–354.

Sun, X. and Doner, H.E. (1996) An investigation of arsenate and arsenite bonding structures on goethite by FTIR. *Soil Science*, **161**, 865–872.

Sun, X. and Doner, H.E. (1998) Adsorption and oxidation of arsenic on goethite. *Soil Science*, **163**, 278–287.

Sun, X., Doner, H.E. and Zavarin M. (1999) Spectroscopy study of arsenite [AsIII] oxidation on Mn-substituted goethite. *Clays and Clay Minerals*, **47**, 474–480.

Sung, W. and Morgan, J.J. (1981) Oxidative removal of Mn(II) from solution catalyzed by the lepidocrocite surface. *Geochimica et Cosmochimica Acta*, **45**, 2377–2383.

Tolentino, H.C.N., Ramos, A.Y., Alves, M.C.M., Barrea, R.A., Tamura, E., Cezar, J.C. and Watanabe, A. (2001) 2.3 to 25 keV XAS beam line at the LNLS. *Journal of Synchrontron Radiation*, **8,** 1040–1046.

Varentsov, I.M. (1964) *Sedimentary Manganese Ores*. Elsevier Publishing Co., Amsterdam, 119 pp.

Waychunas, G.A., Rea, B.A., Fuller, C.C. and Davis, J.A. (1993) Surface chemistry of ferrihydrite: Part 1. EXAFS studies of the geometry of coprecipitated and adsorbed arsenate. *Geochimica et Cosmochimica Acta*, **57**, 2251–2269.

Waychunas, G.A., Davis, J.A. and Fuller, C.C. (1995) Geometry of sorbed arsenate on ferrihydrite and crystalline FeOOH: Re-evaluation of EXAFS results and topological factors in predicting sorbate geometry, evidence for monodentate complexes. *Geochimica et Cosmochimica Acta*, **59**, 3655–3661.

Weidler, P.G., Luster, J., Schneider, J., Sticher, H. and Gehring, A.U. (1998) The Rietveld method applied to the quantitative mineralogical and chemical characterization of ferralitic soil. *European Journal of Soil Science*, **49**, 95–106.

Young, R. (1993) *The Rietveld Methods.* International Union of Crystallography, Oxford University Press, UK, 300 pp.

Young, R.S. (1971) *Chemical Analysis in Extractive Metallurgy*. Barnes & Noble Inc., New York, 427 pp.

Zouboulis, A.I. and Kydros, K.A. (1993) Arsenic (III) and arsenic (V) removal from solutions by pyrite fines. *Separation Science Technology*, **28**, 2440–2463.

(*Received 3 December 2001; revised 11 October 2002; Ms. 611; A.E. Helge Stanjek*)